



Alexandria University  
**Alexandria Engineering Journal**

[www.elsevier.com/locate/aej](http://www.elsevier.com/locate/aej)  
[www.sciencedirect.com](http://www.sciencedirect.com)



ORIGINAL ARTICLE

# Flexural behaviour and ductility of high strength concrete (HSC) beams with tension lap splice



Magda I. Mousa

*Structural Engineering Department, Faculty of Eng., El-Mansoura University, Egypt*

Received 23 October 2014; revised 12 March 2015; accepted 31 March 2015

Available online 2 May 2015

## KEYWORDS

Beams;  
Tension lap splice;  
High strength concrete;  
Flexure;  
Cracking;  
Ductility

**Abstract** An experimental program has been conducted in order to investigate the flexural behaviour of concrete beams with variable length of tension reinforcement lap splice. A test series of eighteen simple beams containing different lap splice length (0, 300, 500 and 700 mm) had been conducted in this investigation. The tested beams are of 2200 mm total length and 200 × 150 mm cross-section, loaded at the middle third with two equal concentrated loads. The parameters included in the experimental program are the splice length, the bar diameter (12, 16 mm), the amount of transverse reinforcement provided within the splice zone, the shape of the anchor at the splices end and the concrete cover (20, 35 mm). The test program has been performed on two grades of high strength concretes (0%, 15% silica fume); 55, 65 MPa. Two deformed bars of tension reinforcement were spliced in the constant moment zone. The effect of splicing tension reinforcement on the response, cracking load, crack propagation, deflection, ultimate capacity, mid-span reinforcement strain, failure mode and beam ductility, is examined. Results show that by introducing an appropriate amount and distribution of transverse reinforcement, a satisfactory ductility response can be obtained (91% of reference beam).

© 2015 Production and hosting by Elsevier B.V. on behalf of Faculty of Engineering, Alexandria University. This is an open access article under the CC BY-NC-ND license (<http://creativecommons.org/licenses/by-nc-nd/4.0/>).

## 1. Introduction

Bond between concrete and tension reinforcement is a major problem in reinforced concrete (RC) structures, which affects the strength and safety. The bond strength of spliced bars in concrete depends on several factors such as concrete cover, bar spacing, bar casting position, development/splice length, bar diameter, bar surface deformation and condition (coated or un-coated), shape of splice end, yield strength, and embedment length of reinforcing bars, concrete compressive and

tensile strength, and mix additives such as silica fume or fibres, aggregate type and quantity, concrete slump and workability admixtures, environment conditions, and loading conditions, the amount of transverse reinforcement provided in the splice or development region [1–9]. Because of the complexity and the effect of a variety of parameters, researchers have not been able to include theoretically all parameters in their assessments of bond. They rather have tried experimental solutions by trial and error procedures and engineering judgment in order to overcome the problem.

Advances in the production, application and utilisation of reinforced concrete have lead to the development of High Performance Concrete (HPC). A common form of HPC is

Peer review under responsibility of Faculty of Engineering, Alexandria University.

<http://dx.doi.org/10.1016/j.aej.2015.03.032>

1110-0168 © 2015 Production and hosting by Elsevier B.V. on behalf of Faculty of Engineering, Alexandria University.

This is an open access article under the CC BY-NC-ND license (<http://creativecommons.org/licenses/by-nc-nd/4.0/>).

High-Strength Concrete (HSC), which can be obtained by minimizing the water–cement ratio with the aid of superplasticizers and carefully selecting reasonable doses and types of pozzolanic admixtures such as silica fume and fly ash.

Results of tests on bond between concrete with compressive strength near or exceeding 70 MPa and reinforcing bars spliced in the tension zone have become available recently [10–15]. The bond strength between deformed rebar and concrete in practical applications is dominated by the steel rib bearing effect on concrete in addition to the adhesion and friction at the steel–concrete interface. In most of the previous studies on HSC, the parameter of concrete compressive strength was investigated, but the possible variation caused by silica fume, SF, on the concrete bond strength and ductility was not clearly reported by researchers [13].

Recent studies have shown that the design provisions of current codes can evaluate the bond strength of lap-spliced concrete beams with reasonable accuracy. However, they fail to fulfil a satisfactory ductility criterion for these beams. It has been shown that, to improve the ductility response of these beams, some transverse reinforcement should be provided over the splice length. However, the required transverse reinforcement which results in an adequate ductility for the spliced-beams has not been presented.

Orangun et al. [6] proposed an empirical equation for bond strength prediction, based on the results of different series of experimental works. The equation later became the basis of the ACI Committee 318-95 [16] equation for the bond strength of spliced bars. It was found from later studies that the ACI equation fails to satisfy the ductility requirement of flexural beams except when the reinforcing ratio  $\rho < \rho_{\max}$  (the maximum value) [9]. The current code provisions do not satisfy the ductility requirement for beams with lap-splice [9,17]. Azizinamini et al. [17] concluded that some transverse reinforcement should be provided over the splice length in order to improve the ductility of beams.

Azizinamini et al. [9] proposed an index ( $i$ ) to represent the displacement ductility ratio in order to assess the ductility of lap-spliced RC beam specimens. It is defined as the ratio of the maximum mid-span displacement over the first yield displacement of beam, Eq. (1). The first yield displacement,  $\Delta_y$ , corresponds to the intersection of the tangents to the load displacement curve at the origin and maximum displacement,  $\Delta_{\max}$ . Therefore, the use of displacement–ductility ratio presents a new criterion in addition to the strength criterion for predicting the behaviour of lap-spliced reinforced concrete beams.

$$i = \frac{\Delta_{\max}}{\Delta_y} \quad (1)$$

Azizinamini et al. [9] showed in their studies that, some specimens failed in a very brittle and violent manner without exhibiting ductility although it had splice length greater than that required by the ACI Committee 318-95 equation and satisfied the bond strength criterion of  $u_{\text{test}}/u_{\text{ACI}} > 1$ . This was attributed to a lack of transverse reinforcement used over the splices. The definition of the yield displacement causes difficulty since the load–displacement may not have a well defined yield point; this may be attributed to the nonlinear behaviour of the materials or the occurrence of yield in different parts at different load levels. The yield displacement  $\Delta_y$  has been recognized as the displacement at 0.75 of the ultimate load [18].

Since the displacement at peak load does not necessarily represent yielding of reinforcement, the term  $\Delta$  is used here instead of  $\Delta_y$ .

In this research, the main objective was to investigate the bond strength and ductility of spliced tension bars in high strength concrete beams. The lap splice is introduced in the tension zone of constant moment and with varied reinforcement bar size and length. This investigation is carried out in terms of flexural crack pattern, cracking and ultimate loads, deflection, steel strain and displacement ductility. The effect of different factors such as transverse stirrups, shape of splice ends, bar diameter, concrete cover as well as introducing silica fume into concrete, on bond strength and displacement ductility is investigated.

## 2. Experimental work

### 2.1. Specimens description

A total of eighteen concrete beams were fabricated and tested in this experimental program. The proposed program consisted of six groups. The objective of this program was to study the effect of different factors such as; tension lap splice length, addition of silica fume (SF) in concrete, lap splice confinement by transverse stirrups, the hooked anchor shape at the splice ends, reinforcement bar size and concrete cover, on the beam flexural behaviour under static loading. The dimensions of the tested beams were 2200 mm length  $\times$  200 mm height  $\times$  150 mm width. The tested beams were simply supported and loaded with two equal point loads at the middle third of the span (Fig. 1). The bottom longitudinal tension reinforcement was two high grade steel bars spliced – if any – in the constant moment zone. The details of the specimens in each group are shown in Table 1 and Fig 2. The first group (1) consists of four beams having different splice length (0, 300, 500, 700 mm) and concrete strength,  $f_{\text{cu}} = 55$  MPa (mix without SF) and bar diameter 12 mm for longitudinal tension reinforcement. The second group (2) is similar to the first group except that, the strength of the concrete mix with 15% SF,  $f_{\text{cu}} = 65$  MPa. In the constant moment region, some specimens had transverse reinforcement in order to study the lateral confinement effect on the splice behaviour as in the third group (3). This group consists of two beams (B5, B6) which are similar to the beam with splice length of 500 mm in group (2) except having uniform transverse reinforcement stirrups along the beam length, 13 $\phi$ 6/2200, (provide three sets along the splice length as in B5) and more additional stirrups

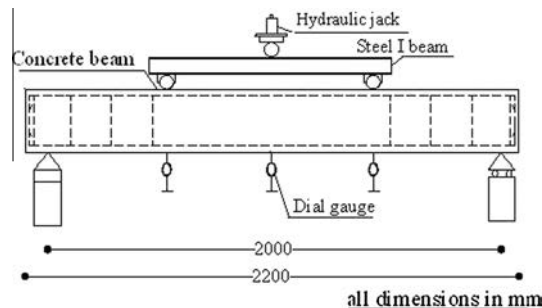


Figure 1 Dimension and details of test beam.

**Table 1** The details of tested beam in each group.

Group	Beam designation	$f_{cu}$ (MPa)	Splice length, $L_s$ (mm)	Bar dia. (mm)	Stirrups no. at lap zone	Splice end	Concrete cover (mm)
1	A1 <sup>ws</sup>	55	–	12	Without	No splice	20
	A2	55	300 (25Ø)	12	Without	Not hooked	20
	A3	55	500 (41.67Ø)	12	Without	Not hooked	20
	A4	55	700 (58.33Ø)	12	Without	Not hooked	20
2	B1 <sup>ws</sup>	65	–	12	Without	No splice	20
	B2	65	300 (25Ø)	12	Without	Not hooked	20
	B3	65	500 (41.67Ø)	12	Without	Not hooked	20
	B4	65	700 (58.33Ø)	12	Without	Not hooked	20
3	B5	65	500 (41.67Ø)	12	3 stir.*	Not hooked	20
	B6	65	500 (41.67Ø)	12	7 stir.**	Not hooked	20
4	B7	65	500 (41.67Ø)	12	Without	Hooked (U shape)	20
	B8	65	500 (41.67Ø)	12	Without	Hooked (bent)***	20
5	B9 <sup>ws</sup>	65	–	16	Without	No splice	20
	B10	65	300 (18.75Ø)	16	Without	Not hooked	20
	B11	65	500 (31.25Ø)	16	Without	Not hooked	20
	B12	65	700 (43.75Ø)	16	Without	Not hooked	20
6	B13 <sup>ws</sup>	65	–	12	Without	No splice	35
	B14	65	500 (41.67Ø)	12	Without	Not hooked	35

ws: refer to the beam without splice.

\* 3 stirrups distributed over the splice length.

\*\* 3 stirrups concentrated at each end of the splice + one at the middle.

\*\*\* Bent with 45° and 200 mm length.

(two stirrups) provided at each end of the splice as in (B6). B7, B8 have splice length of 500 mm which hooked at the end with two different shapes (U shape, bent ends) as in group (4). The fifth group (5) consists of four beams similar to group (2) except using bar diameter of 16 mm instead of 12 mm. The sixth group (6) consists of two beams (B13, B14) similar to group (2) except having concrete side and bottom cover of 35 mm instead of 20 mm and B13 does not have splice whilst B14 has a splice length of 500 mm only (see Table 1).

## 2.2. Material and mix proportions

Ordinary Portland cement (ASTM Type I) was used for producing the concrete mix employed in this program. The fine aggregate used was natural siliceous sand with a fineness modulus of 2.6 and specific gravity 2.63. However, the coarse aggregate was gravel of 20 mm nominal maximum size. The superplasticizer used was the sulphated naphthalene formaldehyde condensate type. The considered silica fume (SF) used contains a silica (SiO<sub>2</sub>) of 95% and was 15% of cement weight in mix M<sub>2</sub>. The concrete mixes chosen for casting the tested beams were designed to be high strength concretes and the proportions are presented in Table 2. The compressive strength ( $f_{cu}$ ) was tested for 150 mm cubes and at least six specimens were tested for each mix. The following mean values were obtained:  $f_{cu} = 55$  MPa, and 65 MPa for mixes M1 and M2, respectively.

For the reinforcement, three specimens were tested for every bar diameter. The longitudinal reinforcement in tension consisted of two deformed bar sizes, 12 and 16 mm nominal diameters, either spliced or not (control beam) at the middle third of the bottom of the beam, with an average yield stress,

$f_y = 498$  MPa. The longitudinal compression reinforcement at the top of the beam consisted of two ribbed bars of 10 mm diameter, with an average yield strength of 427 MPa. Plain round bars of 6 mm diameter with an average yield stress of 300 MPa were used as stirrups.

## 2.3. Specimen preparation and test procedure

In order to carry out this experimental program, moulds manufactured of wood with internal dimensions of 150 mm × 200 mm × 2200 mm were used in casting eighteen high strength concrete beams reinforced with high grade steel bars. The moulds were stiff enough to prevent any significant movement during placing the concrete. Before casting the specimens, electrical resistance strain gauges (with 120 Ω resistance) were installed to measure the strain in the middle of the two longitudinal tension bars either spliced or not. The strain gauges were fixed on the steel bars using special glue and then covered with a water proofing material for protection. The specimens were cast in the moulds immediately after mixing the concrete, and then compacted on a vibrating table. The specimens were cast in a horizontal position with the two spliced rebar placed in the bottom of wood forms and were exposed to identical curing conditions. They were stored in the laboratory, then de-moulded after 24 h and covered with wet burlap and plastic at room temperature for 28 days.

The beams were tested under 4-point static loading (Fig. 1). A hydraulic jack was to apply the static load with an increment of 5 kN until failure. At each stage the load was kept constant for about 10 min during each increment whilst the readings were being recorded. Fig. 3 shows the

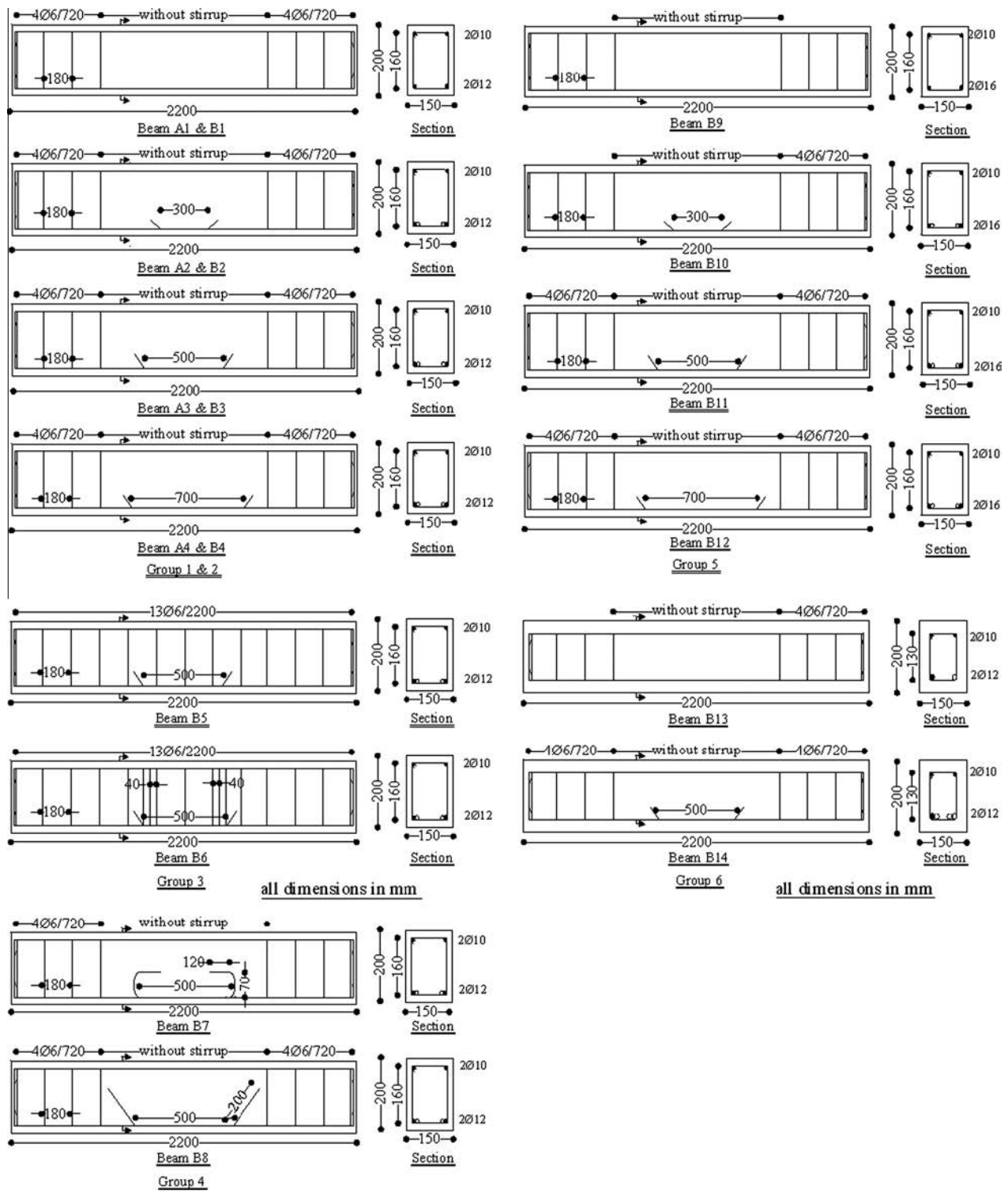


**Figure 2** Details of reinforcement and concrete dimensions of all specimens (groups 1–6).

general arrangement of the test setup of all beams. At each load stage, cracks were marked, the deflection at the middle and one third of the span of the beams was measured (under the applied load) using three deflect metres (dial gauges) with 0.01 mm accuracy and also the strain at the centre of the tension bars was recorded.

#### 2.4. Code provisions for splice length

According to the ECP 203 [19] Eq. (2) proposed for calculating the minimum tension splice length.

$$L_d = [\alpha\beta\eta(f_y/\gamma_s)/(4f_{bu})]\phi \quad (2)$$

**Table 2** Concrete mix proportion (kg/m<sup>3</sup>).

Concrete mix	Cement	Water	Gravel (20 mm)	Sand	Super plasticizer (SP%)	Silica fume (SF%)
M1	500	110	1223	659	15 (3%)	0.0
M2	500	126.5	1152	620	17.25 (3%)	75 (15%)

**Figure 3** Test setup.

where  $\eta = 1$  for splices near bottom surface of beams,  $\eta = 1.3$  for splices near top surface of beams if the beam thickness is greater than 300 mm.  $\beta$  = correction factor for bar surface and is equal to 0.75 for deformed bars,  $\alpha$  = correction factor for bar ends and is equal to 1 for straight bars,  $f_{bu}$  = bond strength of concrete and is equal to  $0.3 \sqrt{f'_c}/\gamma_C$ ,  $f'_c$  is the concrete compressive strength in MPa and  $\gamma_C$  is the concrete strength reduction factor; equals 1.5.

The calculated  $L_d \sim 45\emptyset$ ,  $41.23\emptyset$  for  $f'_c = 55$ , 65 MPa, respectively.

The ACI 318-11 [20] proposed the following equation for calculating the lap splice length.

$$L_d = (f_y \psi_t \psi_e \lambda / 2.1 \sqrt{f'_c}) \emptyset \quad (3)$$

where  $\psi_t = 1.0$  for bottom cast beams (splice near the bottom surface of the beam) and  $\psi_t = 1.3$  for top cast beams,  $\psi_e \times \psi_t$  should not less than 1.7.  $\psi_e = 1.0$  for uncoated reinforcement, and  $\lambda = 1.0$  for normal weight concrete. According to the ACI code the required splice length =  $55\emptyset$ ,  $50\emptyset$  for  $f'_c = 55$ , 65 MPa, respectively.

In this study the shortest splice length of these calculated by codes was considered in beam B<sub>3</sub> ( $L_d = 500$  mm,  $41.67\emptyset$ ). This basic splice length was reduced by about 40% in beam B<sub>2</sub> ( $L_d = 300$  mm), and increased by about 40% in beam B<sub>4</sub> ( $L_d = 700$  mm). Beam B<sub>3</sub> has been utilised to study the other parameters such as the effect of transverse stirrups over the splice length, effect of hooks shape at the splice ends, and the cover thickness of reinforcement, on the flexural beam behaviour.

### 3. Test results and discussion

#### 3.1. Cracking and ultimate loads

Table 3 gives the cracking, failure loads of the investigated beams. Regarding to the effect of splice length, the cracking

**Table 3** Test results of different beams in each group.

Group	Beam designation	Cracking load, P <sub>cr</sub> (kN)	Ultimate load, P <sub>u</sub> (kN)	$\Delta_e$ (mm)	$\Delta_u$ (mm)	Deformability $i = \Delta_u/\Delta_e$	Ductility (D), inelastic P- $\Delta$ area (kN mm $\times 10^2$ )	$D/D^{ws}\%$	Failure mode*
1	A1 <sup>ws</sup>	30	75	6.67	38.0	5.70	20.55	100	Fl.
	A2	27	70	5.67	17.89	3.16	6.10	32.12	Sp.
	A3	30	72.5	5.67	19.1	3.00	7.00	37.00	Fl.
	A4	30	75	5.67	21.31	3.56	8.26	46.32	Fl.
2	B1 <sup>ws</sup>	27	75	8.00	37.64	5.38	19.14	100	Fl.
	B2	25	67.5	5.67	16.5	2.90	5.53	36.00	Sp.
	B3	27	72.5	6.00	17.95	2.99	6.89	37.47	Fl.
	B4	27	75	6.33	20.0	3.33	7.75	43.26	Fl.
3	B5	35	75	6.33	30.83	4.62	14.9	77.85	Fl.
	B6	40	76	6.00	32.0	4.90	16.57	86.57	Fl.
4	B7	30	81	6.33	22.2	3.51	11.30	62.48	Fl.
	B8	30	75	6.33	20.86	3.30	10.54	55.31	Fl.
5	B9 <sup>ws</sup>	45	125	10.33	16.92	1.64	7.70	100	Sh/Fl
	B10	35	105	7.00	10.96	1.57	1.58	20.52	Sp.
	B11	35	111	6.33	10.3	1.63	2.21	28.70	Sh/Fl
	B12	40	125	9.67	15.27	1.58	5.44	70.65	Sh/Fl
6	B13 <sup>ws</sup>	20	70	10.33	30	2.90	10.87	100	Fl.
	B14	20	68	6.00	12.1	2.02	3.04	28.00	Fl.

ws: refer to the beam without splice in each group.

$D/D^{ws}$ : ductility of the beam/ductility of the similar reference beam without splice.

Failure mode\*: Fl = Flexural, Sp = Splitting, Sh/Fl = Shear/Flexural.

load ( $P_{cr}$ ) reduced by about 10%, 7.4%, and 11% for short splice length of 300 mm in groups 1, 2 (25Ø) and group 5 (18.75Ø) whilst the reduction in the ultimate load ( $P_u$ ) was 6.7% and 16%, respectively, compared with similar reference. For splice length of 500 mm there was no reduction in  $P_{cr}$  and only 3% in  $P_u$  for A3, B3 in group 1, 2 whilst, the reduction for B11 in group 5 was 11% in both  $P_{cr}$  and  $P_u$  with respect to their reference beam. Increase the splice length to 700 mm, almost the reduction in  $P_{cr}$  and  $P_u$  vanished for A4 and B4, whilst a decrease of about 11% recorded in  $P_{cr}$  for B12 compared to corresponding reference beam (B9).

Comparing the results of  $P_{cr}$  and  $P_u$  for specimens in group 1 with respect to the specimens in group 2 (the mix with SF) it can be observed that, the dose of 15% SF relatively has no effect on the ultimate load whilst reduce the cracking load by about 9% for reference and spliced beams.

The presence of transverse stirrups distributed or concentrated at the splice ends (B5, B6), increases significantly  $P_{cr}$  by about 29.6%, 48.2% whilst has minor effect of 3.5%, 4.8% on  $P_u$  relative to similar beam without stirrups (B3).

The hooked located at the splice ends affect positively in increasing  $P_{cr}$  and  $P_u$  of the beam. The increase was about 11% in cracking load, whilst the increase in the ultimate load was 12% and 3.5% for the splice ends hooked in u-shape (B7) and the bent ends (B8), respectively, compared with straight splice in B3.

Comparing the results of group 2 and 5 given in Table 3 indicate a significant increase in  $P_{cr}$  and  $P_u$  due to increasing the bar diameter from 12 mm to 16 mm (reinforcement ratio from 0.755 to 1.34). The increase in both cracking and failure loads was 66.7% for the reference beam (B9), whilst in spliced beams was 32%, 30%, 48% and 50%, 55%, 66.7% for B10, B11 and B12, respectively.

The increase in concrete cover at the side and bottom of reinforcement from 20 mm in specimens (B1, B3) to 35 mm in specimens of group 6 (B13, B14) reduces both the cracking and the ultimate loads (Table 3). The reduction recorded in  $P_{cr}$  was 26% whilst in  $P_u$  was 6.7% and 6.2% for B13 and B14 compared with B1 and B3, respectively.

### 3.2. Crack propagation

Fig. 4 shows the crack pattern of all studied beams. The number given along each crack represents the load at which the crack was extended. Considering the two groups 1 and 2 of concretes without and with SF, respectively, the reference beams (A1, and B1) shows flexural cracks distributed along the beam length. Regarding the effect of the splice on the crack propagation, flexural cracks started at the free ends of the spliced bars where the ends act as crack initiators due to the high stress concentration and in turn longitudinal (splitting) cracks developed in the beam cover due to the radial components of the anchorage forces; then the concrete cover failed. This mode of failure was explosive with high sound which took place in beams A2, and B2 with splice length of 300 mm, 25Ø, under the values recommended by codes. The use of small cover in these beams (20 mm, bottom and side cover) attained splitting rather than pull-out failure since the area of concrete surrounding cannot sustain the circumferential tensile stresses. Generally, it is observed that the region of lap splice was free of cracks with the exception of one or two small cracks as in

beams A3, and B3 with splice length 500 mm (41.67Ø). On the other hand, when the splice length increased to 700 mm (58.33Ø) the cracks existed along the splice as noted in beams A4, and B4. Comparing the beams of group 1 with the corresponding beams of group 2 indicates that the addition of silica fume did not affect either the crack pattern or failure mode (Fig. 4).

The crack pattern due to flexural failure of specimens with stirrups over the splice length (B5 and B6) was relatively more in number, especially across the splice area, compared to the specimen without stirrups (B3) and as the number of stirrups increased the number of cracks along the splice increased with better distribution. Transverse steel improves the bond strength and ductility of the anchorage [6] thereby the cracks are more evenly distributed.

The crack pattern of beams B7 and B8 shows the effect of hooked splice ends with different shapes (U shape or bent up with 200 mm length) on the efficiency of the anchorage. The number of cracks increased and they are better distributed especially in B7 indicating higher ductility of the beam.

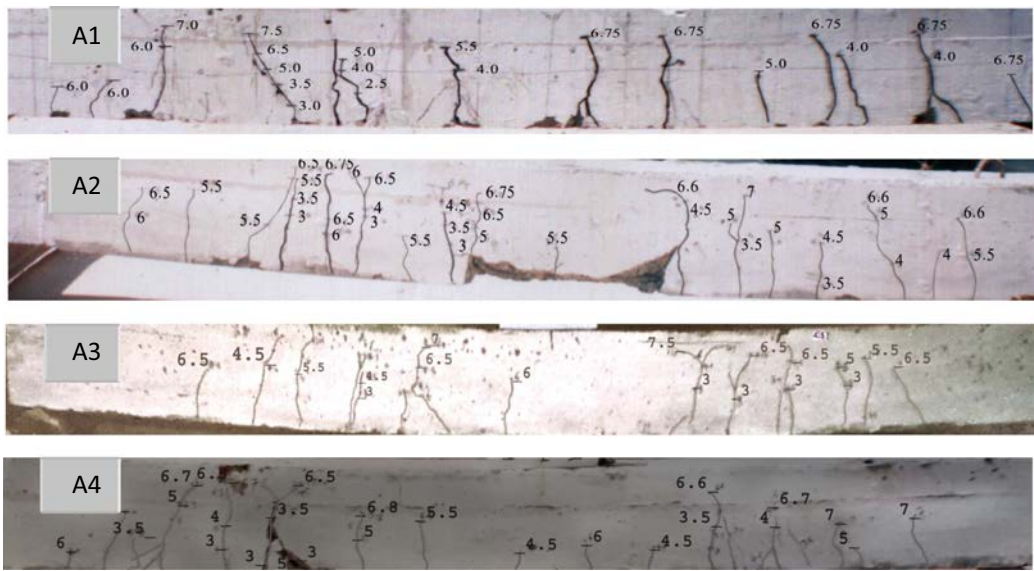
For beams in group 5 (B9–B12) with larger bar diameter (Ø16), the number of cracks was smaller compared to the corresponding beams in group 2 with Ø12 (B1–B4) and the spliced zone was almost free from flexural cracks. All the beams in this group showed shear–flexural failure mode, except B10 with splice length 300 mm (18.8Ø) where failure occurred due to a longitudinal splitting crack below the splice region and it was sudden and brittle.

Increasing the concrete cover from 200 mm to 350 mm, reduced the number of flexural cracks either in the beam with bars spliced (B14) or not (B13) in comparison with the corresponding beams with 200 mm cover (B3 and B1), respectively, which reflects the reduction in beam ductility.

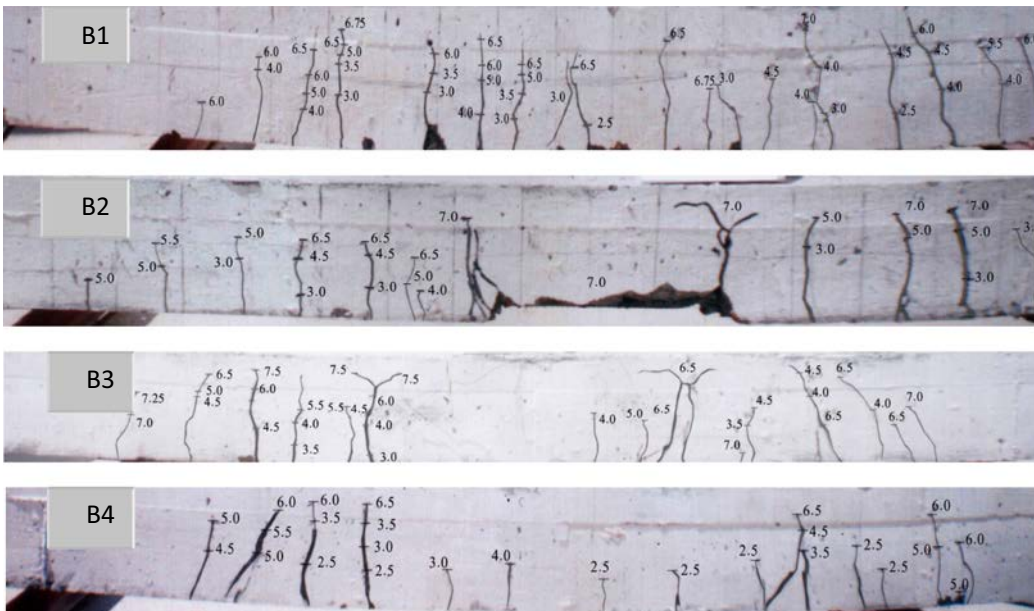
### 3.3. Load deflection and load strain behaviour

The load–central deflection curves of the different beams are shown in Figs. 5–12. Generally, the load–deflection curves can be classified to three distinct zones; the first zone is the initial part of the curve up to the cracking point, the post-cracking zone, continued up to the yielding point, and the post yield zone, up to failure. At the initial stage the beams stiffness showed almost identical histories at low level of loading and up to the cracking load, as this stage is controlled mainly by the concrete tensile strength. The second zone, showed a distinct behaviour in the different beams. The slope of the curve in this zone is almost linear and of crucial importance in design, it is a direct function which represents the effective stiffness of the beam. Regarding the post yield zone, the beams showed the ability to withstand higher load in different rates and to gain more deformability until failure.

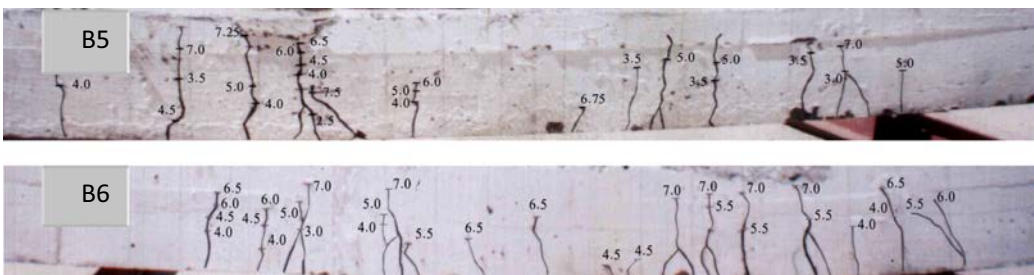
Figs. 5 and 6 show the load–deflection curves of groups 1 and 2, respectively. After the cracking stage, the beams with different lap splices length (A2, A3, A4 and B2, B3, B4) showed higher stiffness (which is more pronounced in group 2) than their corresponding control beam without splice (A1 and B1). The increase in spliced beam stiffness is a result of the extent of the reinforcement with double the cross-sectional area. As illustrated by the load–strain relations in Figs. 5b and 6b, no yielding was observed in the steel rebar of specimens which showed splitting failure (A2 and B2)



Group 1



Group 2



Group 3

**Figure 4** Crack pattern and failure mode for tested beams.

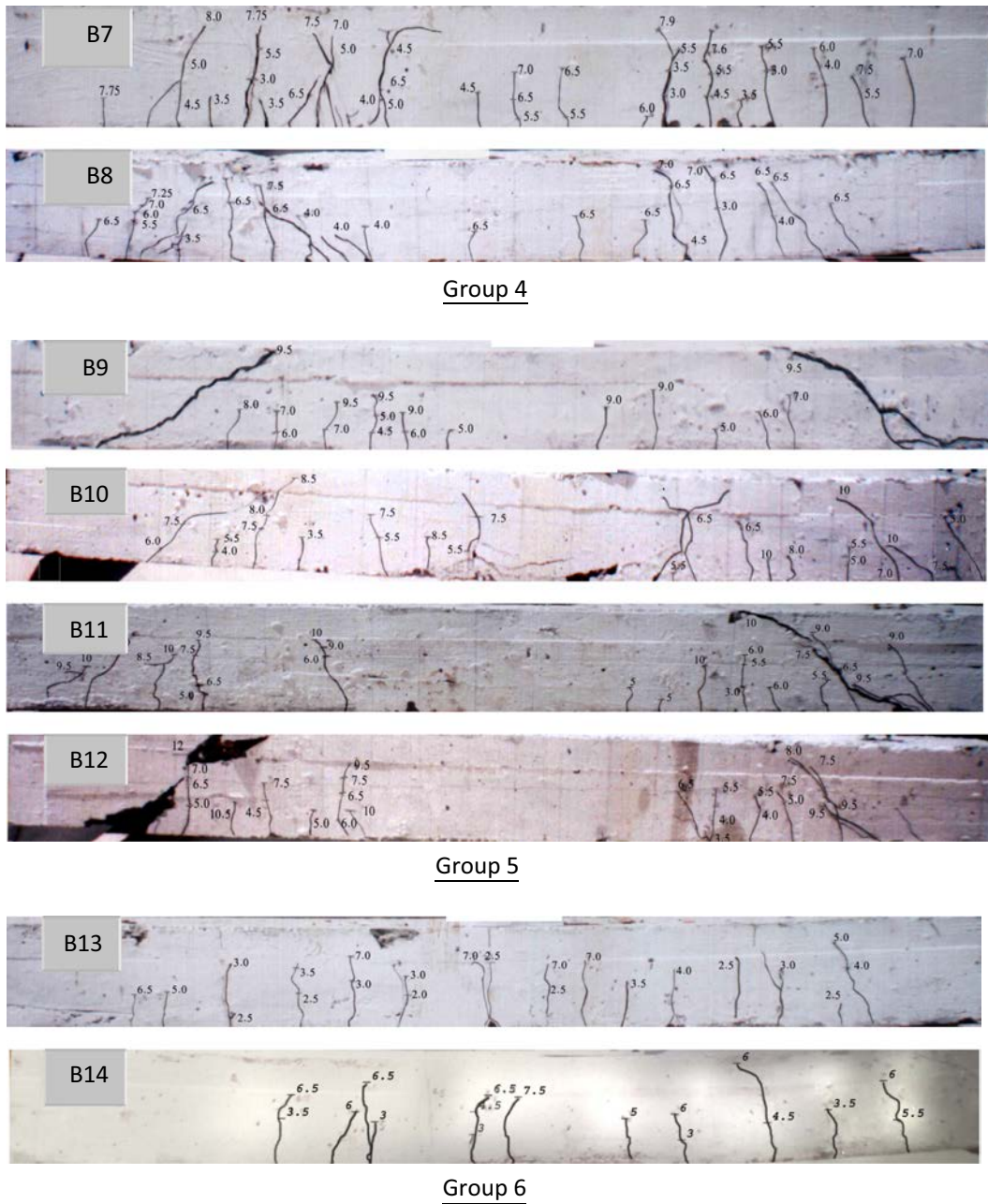


**Figure 4** (continued)

whilst, the remaining beams showed yielding in steel (producing flexural failure). Figs. 7a and 7b show the effect of 15% SF addition on the load deflection behaviour of the beams. The stiffness and the ultimate deflection slightly decreased, the maximum reduction was about 7.8% in the beam which exhibited splitting failure.

The presence of transverse stirrups in the splice zone had minor influence on the beam stiffness (Fig. 8). However, using transverse stirrups over the splice length, distributed or concentrated at the ends of the splice (B5 and B6), was more efficient in increasing the ultimate deflection compared to the similar beam without stirrups (B3). The beam with concentrated stirrups (three stirrups at each end, B6), showed the highest ultimate deflection, somewhat closer to the

reference beam without splice, with about 85% of that of B1, Table 3. In this group, the beams exhibited yielding of longitudinal steel as indicated in the load-strain relationship (Fig. 8b).

The effect of the shape of lap-splice bar ends on the load-deflection relationship is shown in Fig. 9a. This effect can be noticed from the yielding point to failure, where the stiffness and the ultimate deflection increased 24% in the beam with hooked ends splice in U shape (B7) compared to the similar beam without hooks at the splice ends (B3). The load-strain curves also confirmed yielding of steel rebar in this group as shown in Fig. 9b. The maximum strain of the beam with hooked ends particularly U shaped is significantly the largest compared to the beam without hooked or with bent ends

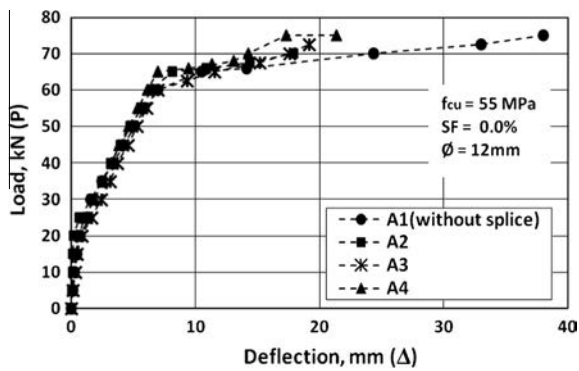


Figure 5a Effect of splice length on load–deflection relationship (group 1).

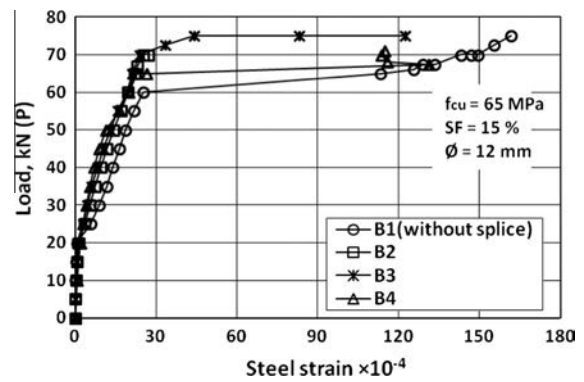


Figure 6b Load–steel strain relationship (group 2).

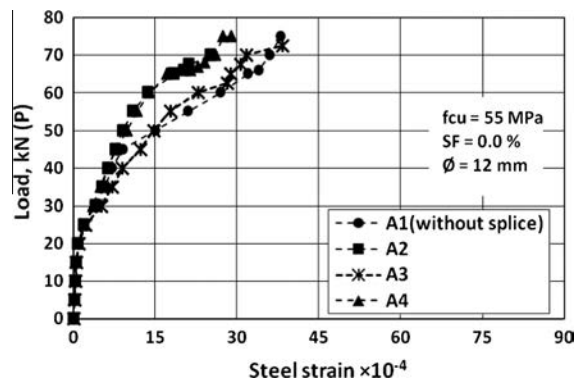


Figure 5b Effect of splice length on load–steel strain relationship (group 1).

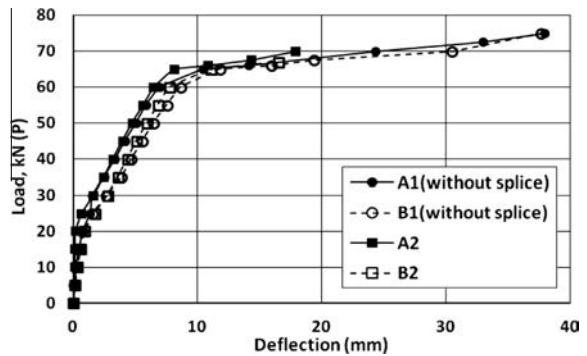


Figure 7a Load–deflection relationship for group 1, 2 ( $L_S = 0, 300$  mm).

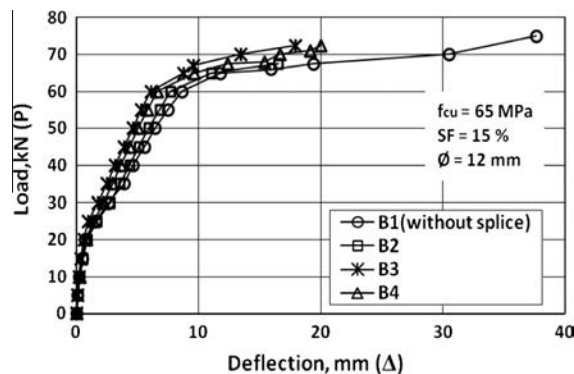


Figure 6a Load–deflection relationship (group 2).

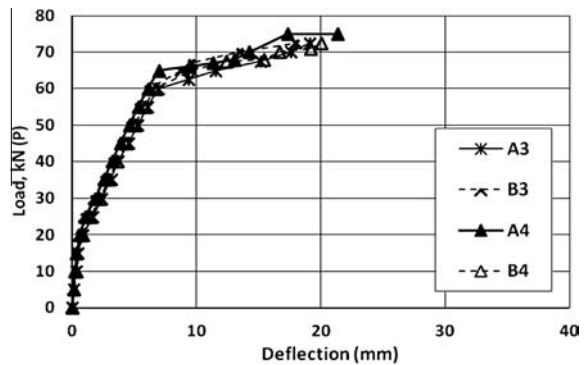


Figure 7b Load–deflection relationship for group 1, 2 ( $L_S = 500, 700$  mm).

splice, which indicates a more effective transfer of stress from concrete to the steel rebar via hooked ends in U shape.

Figs. 10a and 10b show the relationship between the load versus deflection and steel strain, respectively, for group 5. In general, all the spliced beams showed an increase in the stiffness compared with their reference beam without splice. The beam (B12) with 700 mm (43.8Ø) splice length showed similar behaviour and around 90% ultimate deflection of the corresponding reference beam without splice (B9). As illustrated by the load–strain curves in Fig. 10b no yielding was observed

in the steel rebar of these specimens, due to the inadequacy of shear reinforcement.

For the purpose of comparison and to illustrate the effect of bar diameter on the load–deflection relationship, subgroups, consist of beams with bar diameter Ø16 (B9, B10), (B11, B12) and their corresponding beams with bar diameter Ø12 (B1, B2), (B3, B4), respectively, were considered and shown in Figs. 11a and 11b. The figures show that, the increase in bar diameter significantly increases the stiffness of the beams (B9–B12) and the ultimate load compared to the similar beams

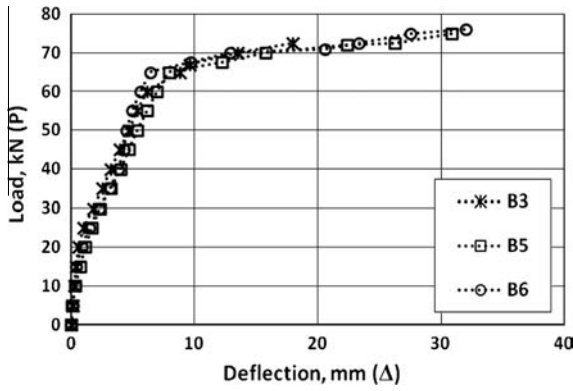


Figure 8a Load-deflection relationship (group 3).

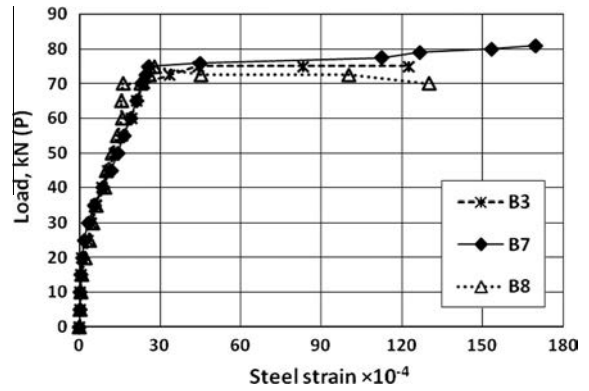


Figure 9b Load-steel strain relationship (group 4).

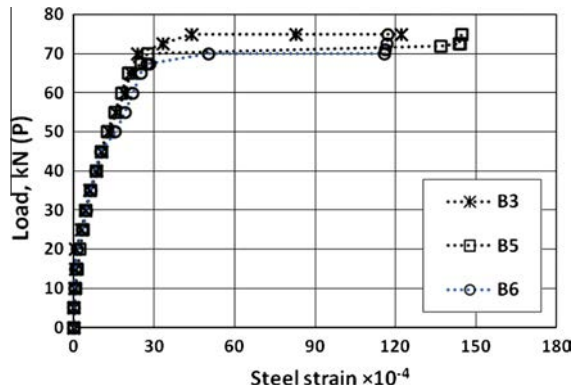


Figure 8b Load-steel strain relationship (group 3).

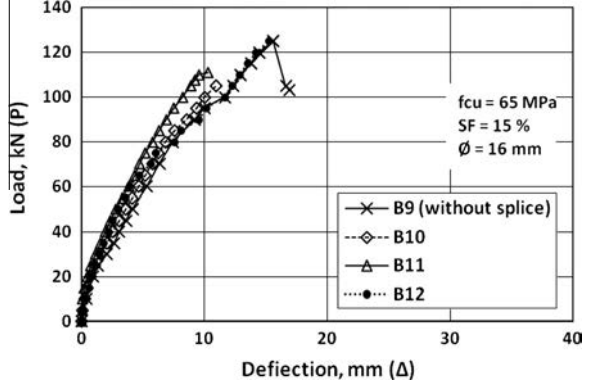


Figure 10a Load-deflection relationship (group 5).

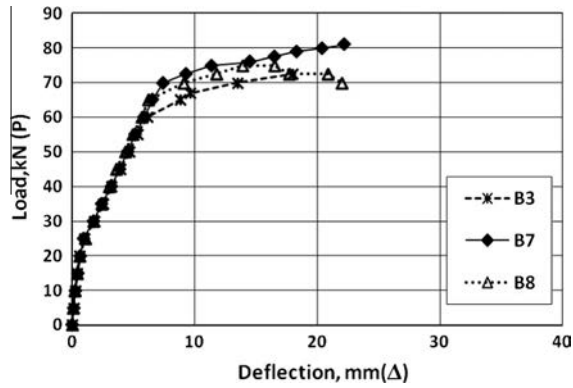


Figure 9a Load-deflection relationship (group 4).

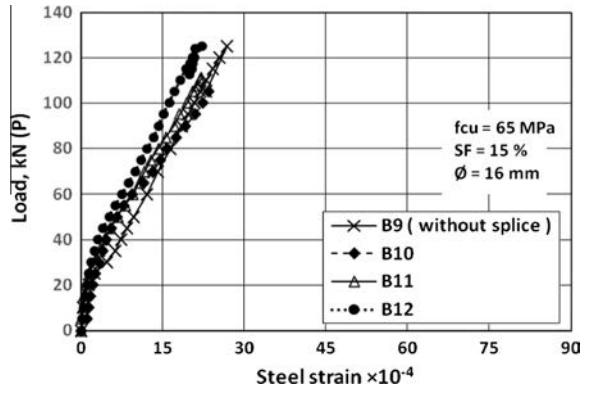


Figure 10b Load-steel strain relationship (group 5).

with smaller bar diameter (B1–B4), the deflection was smaller at the same load. The results obtained from beams with bar diameter 16 mm have ultimate deflection less than that of similar beams with bar diameter 12 mm.

The effect of increasing concrete cover over the steel reinforcement on the load-deflection relationship of group 6 (B13, B14 with concrete cover 35 mm) and their similar beams with concrete cover 20 mm (B1, B3), is illustrated in Fig. 12. Increasing the concrete cover in the side and bottom of the reinforcement from 200 mm to 350 mm decreased significantly the stiffness and the ultimate

deflection, the ultimate deflection of spliced beam (B14) was reduced to 67% of B3.

### 3.4. Ductility and deformability

Two approaches have been utilised in this study in order to describe flexural ductility of beams. The first by calculating the inelastic deformation area under the  $P-\Delta$  curve and the second through the displacement ductility/deformability index,  $i = \Delta_u/\Delta_e$ . The ductility of the studied beams using the two approaches is shown in Table 3.

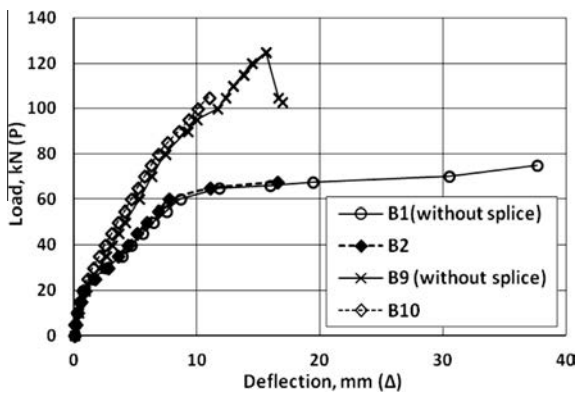


**Figure 11a** Load–deflection relationship for group 2, 5 ( $L_S = 0$ , 300 mm).

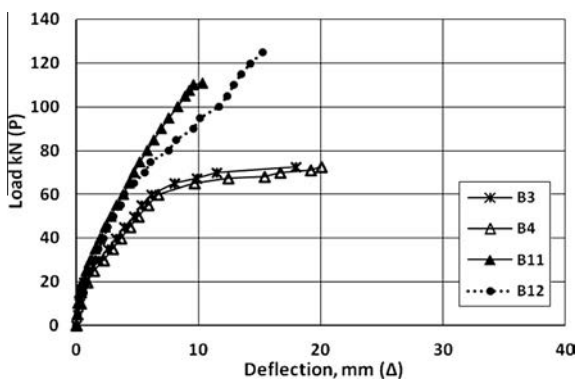


**Figure 11b** Load–deflection relationship for group 2, 5 ( $L_S = 500$ , 700 mm).

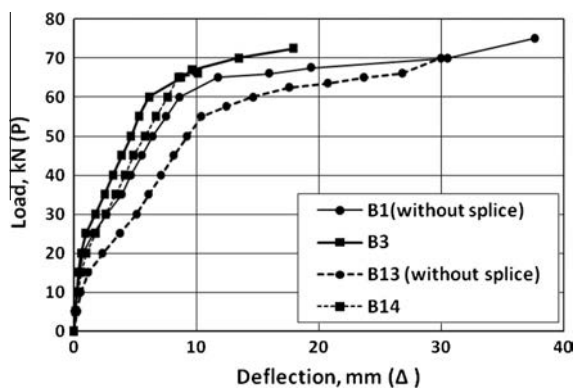


**Figure 12a** Load–deflection relationship (group 6).

In general, all the specimens with tension lap splices showed higher reduction in ductility (the inelastic area under  $P-\Delta$  curve, the index  $i$ ) when compared with their corresponding reference without splice. In spite of increasing the splice length to around  $58\phi$  as in A4, B4 (40% increase of recommended code), it was observed that the deformability index  $i$  of the beam increased only to about 62% of the similar reference beam. This observation is due to the non-attendance of the transverse stirrups over the splice length.

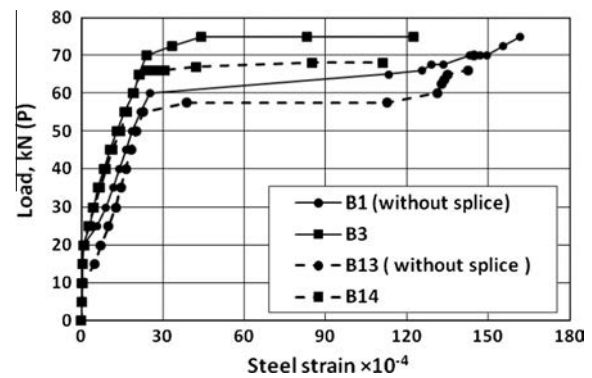


**Figure 12b** Load–steel strain relationship (group 6).

The displacement–ductility of silica fume specimens (group 2) decreased compared with plain cement specimens in group 1, 8% maximum reduction recorded in ductility ratio ( $i$ ) in the beam with concrete splitting failure (B2).

The deformability ratios of beams which have transverse stirrups over the splice length (B5, B6) were much higher than that of the corresponding beam without stirrups B3 ( $i = 4.62, 4.9, 2.99$  for B5, B6, B3, respectively). It is seen that the ductility of beam B5 (have 3 stirrup over the splice length) is satisfactory in comparison with the reference beam without splice B1 (its ductility is about 86% of B1). Furthermore, the beam with concentrated stirrups B6 (three stirrups at each end) showed ductility ratio ( $i$ ) somewhat closer to the reference beam without splice B1, with about 91% of B1.

The spliced beams with hooked ends in U shape or bent, B7 and B8 gave ductility ratio higher by about 17.4%, 10.4% than similar beam without hooked ends B3, it represent about 65.24%, 61.34% of reference beam without splice.

The effect of bar diameter increase (from  $\phi = 12$  mm to 16 mm) on the deformability ratio can be carried out through a comparison of the results of groups 2, 5 in Table 3 and Figs. 11a and 11b. The deformability ratio decreased markedly as obvious in B10 ( $L_S = 300$  mm– $18.8\phi$  and failed by splitting of concrete cover), it was about 54.14% of B2. The reduction in the ductility of beams B9, B11, B12 was due to increasing the bar diameter along with less shear reinforcement in the shear zone which caused early shear–flexural failure.

Increasing the concrete cover in the sides and over the reinforcement from 200 mm to 350 mm reduced markedly the ductility ratio, it represent about 53.9%, 67.56% of that of the beam without and with spliced bars B13 and B14, respectively, compared to similar beams with smaller cover B1 and B3. Calculating the ductility by the inelastic area under  $P-\Delta$  curve relatively produces somewhat similar behaviour and ratios.

#### 4. Conclusions

To evaluate the effect of different parameters on the efficiency of the beams with rebar spliced at the mid-third of the beam and subjected to flexural load, 18 beam splice specimens were cast and tested. The bond strength was investigated in terms of cracking, ultimate loads and failure mode, deflection, strain, and ductility of the HSC beams. Based on the experimental results, the following conclusion can be drawn:

- (1) Splitting failure of the concrete specimens reinforced with 12 mm bar diameter and with splice length 300 mm (25 $\emptyset$ ) was sudden, violent and occurred along the entire length of the splice. It is recommended to use minimum transverse reinforcement within the splice zone to confine the failure and to control propagation of splitting cracks. On the other hand, the specimens of splice length 500 mm ( $\sim$ 42 $\emptyset$ ) and more showed flexural failure.
- (2) The presence of 15% silica fume in concrete caused minor reduction in stiffness in some specimens. Cracking and ultimate loads, ultimate deflection and the ductility ratio reduced with small percentages. The maximum reduction in the displacement–ductility was about 8% in the beam which exhibited splitting failure. This may be attributed to the loss of adhesion between concrete and steel at the ribs produced from SF, thereby reducing the beam bond strength.
- (3) The confinement provided by transverse stirrups is more effective if they are concentrated at the splice ends, which increases significantly the cracking load and number of cracks with better crack pattern distribution especially in splice area zone. This refers to the enhancement in the bond strength of the splice and the beam ductility. The cracking load and the ductility ratio increased by about 48.2% and 64% for the beam with concentrated stirrups at the splice ends relative to similar beam without stirrups at the splice zone. On the other hand, such a beam was similar in behaviour and ductility (91%) to the reference beam without splice.
- (4) The use of hooked end splice increased the cracking, ultimate loads and the failure was more ductile compared with the similar beam without hooks. The splice with U shape is more effective than the bent shape, the improvement in cracking, ultimate loads and in ductility ratio was 11.11%, 11.7% and 17.4%, respectively, compared to the beam without hooks. Whilst, compared to the reference beam without splice the increase was only 8% in  $P_U$  and the ductility ratio represent 61.34% of the reference. This behaviour reflects the efficiency of transmitting the force between the two bars of the splice of hooked ends.
- (5) Increasing the bar diameter from  $\emptyset$ 12 mm to  $\emptyset$ 16 mm (with increasing reinforcement ratio by about 77.5%) increased markedly the beams stiffness, thereby both cracking and failure loads ( $P_C$ ,  $P_U$ ) increased significantly by about 66.7%, 40%, 29.6% and 48.2% in  $P_C$ ; whilst, by about 66.7%, 55.56%, 53.1% and 66.7% in  $P_U$  for the beams with splice length of  $L_S = 0.0$ , 300 mm, 500 mm and 700 mm, respectively. The ductility ratio ( $i$ ) of the beam failing by splitting decreased by about 45.86% and the other beams exhibited shear–flexural failure.
- (6) The increase in concrete cover in the side and over the reinforcement from 200 mm to 350 mm reduced significantly the number of cracks,  $P_C$ ,  $P_U$ , the stiffness and the ductility of the beam. The reduction recorded in  $P_{Cr}$  was 26% for both beams without and with splice ( $L_S = 500$  mm), and was 6.7%, 6.2% in  $P_U$ , respectively. Whilst the ductility ratio reduced to represent

about 53.9%, 67.56% for the beam without and with spliced bars, respectively, compared to the similar beams with less cover.

### Acknowledgements

The author gratefully acknowledges the support provided by the Department of Civil Engineering, Structural engineering, at El-Mansoura University in particular, as well as the concrete and material laboratories to carry out this work. Moreover, the author would like to thank the prof. Dr. Salah El-Metwally for his assistance in proof reading the paper.

### References

- [1] Chenglin Wu, G. Chen, J.S. Volz, R.K. Brow, M.L. Koenigstein, Global bond behavior of enamel-coated rebar in concrete beams with spliced reinforcement, *Constr. Build. Mater.* 40 (2013) 793–801.
- [2] S.B. Hamad, M.H. Harajli, G. Jumaa, Effect of fiber reinforcement on bond strength of tension lap splices in high-strength concrete, *ACI Struct. J.* 98 (2001) 638–647.
- [3] B.S. Hamad, M.Y. Mansour, Bond strength of noncontact tension lap splices, *ACI Struct. J.* 93 (1996) 316–325.
- [4] L.A. Lutz, S.A. Mirza, N.K. Gosain, Changes to and applications of development and lap splice length provisions for bars in tension (ACI 318-89), *ACI Struct. J.* 90 (1993) 393–408.
- [5] Esfahani MR, Rangan BV. Bond between high-performance concrete (HPC) and reinforcing bars in splices of beams. *ACI Special Publication 1999 – concrete.org.*
- [6] C.O. Orangun, J.O. Jirsa, J.E. Breen, A reevaluation of test data on development length and splices, *ACI J. Proc.* 74 (11) (1977) 114–122.
- [7] R. Aly, Stress along tensile lap-spliced fiber reinforced polymer reinforcing bars in concrete, *Can. J. Civ. Eng.* 34 (9) (2007) 1149–1158.
- [8] T. Rezansoff, S. Zhang, B.F. Sparling, Influence of different stirrup configurations on lap splices in beams, *Can. J. Civ. Eng.* 24 (1) (1997) 106–114.
- [9] A. Azizinamini, R. Pavel, E. Hatfield, S.K. Gosh, Behavior of lapspliced reinforcing bars embedded in high strength concrete, *ACI Struct. J.* 96 (5) (1999) 826–836.
- [10] ACI Committee 318. Building code requirements for reinforced concrete and commentary. American Concrete Institute (ACI) 1995 Detroit. 369pp.
- [11] A. EL-Azab, H.M. Mohamed, Effect of tension lap splice on the behavior of high strength concrete (HSC) beams, *HBRC J* (2014).
- [12] M.A. El-Azab, H.M. Mohamed, A. Farahat, Effect of tension lap splice on the behavior of high strength self-compacted concrete beams, *Alexandria Eng. J.* 53 (2) (2014) 319–328.
- [13] S.J. Hwang, Y.Y. Lee, C.S. Lee, Effect of silica fume on the splice strength of deformed bars of high-performed concrete, *ACI Struct. J.* 91 (1994) 294–302.
- [14] J. Zuo, D. Darwin, Splice strength of conventional and high relative rib area bars in normal and high-strength concrete, *ACI Struct. J.* 97 (2000) 630–641.
- [15] M. Rakhshanimehr, M.R. Esfahani, M.R. Kianoush, B.A. Mohammadzadeh, S.R. Mousavi, Flexural ductility of reinforced concrete beams with lap-spliced bars, *Can. J. Civ. Eng.* 41 (7) (2014) 594–604.
- [16] ACI Committee 318, Building code requirements for reinforced concrete and commentary (ACI 318-95/ACI 318R-95), American Concrete Institute (ACI), Farmington Hills, Mich., 1995.

- [17] A. Azizinamini, D. Darwin, R. Eligehausen, R. Pavel, S.K. Ghosh, Proposed modifications to ACI 318-95 tension development and lap splice for high-strength concrete, *ACI Struct. J.* 96 (6) (1999) 922–927.
- [18] R. Park, Evaluation of ductility of structures and structural assemblages from laboratory testing, *Bull. New Zealand National Soc. Earthquake Eng.* 22 (3) (1989) 155–166.
- [19] ECP No. 203, Egyptian Code of Practice for Design and Construction of Concrete Structures, Housing and Building National Research of Egypt, Giza, Egypt, 2007.
- [20] American Concrete Institute, ACI 318-11 Metric Building Code Requirements for Structural Concrete and Commentary, American Concrete Institute, Farmington Hills, Mich., USA, 2011, 503 pp.